Meteoritics & Planetary Science 37, 549–563 (2002)
Available online at http://www.uark.edu/meteor

Itawa Bhopji (L3–5) chondrite regolith breccia: Fall, classification, and cosmogenic records

N. BHANDARI[1]*, S. V. S. MURTY[1], P. N. SHUKLA[1], A. D. SHUKLA[1], R. R. MAHAJAN[1], M. M. SARIN[1], G. SRINIVASAN[1], K. M. SUTHAR[1], M. S. SISODIA[2], S. JHA[3] AND A. BISCHOFF[4]

[1]Physical Research Laboratory, Ahmedabad 380009, India
[2]J.N.V University, Jodhpur 342005, India
[3]Forensic Sciences Laboratory, Jaipur 302016, India
[4]Institut für Planetologie Wilhelm-Klemm-Strasse 10, D-48149 Münster, Germany
*Correspondence author's e-mail address: bhandari@prl.ernet.in

(Received 2001 August 10; accepted in revised form 2002 January 4)

Abstract–A stony meteorite fell at Itawa Bhopji, Rajasthan, India on 2000 May 30. This is the fifth recorded fall in a small area of Rajasthan during the past decade. The meteorite is an ordinary chondrite with light clasts in a dark matrix, consisting of a mixture of equilibrated (mainly type 5) and unequilibrated components. Olivine is Fa_{24-26} and pyroxene Fs_{20-22} but, within the unequilibrated components, olivine (Fa_{5-29}) and low calcium pyroxene (Fs_{5-37}) are highly variable. Based on petrographic studies and chemical analyses, it is classified as L(3–5) regolith breccia. Studies of various cosmogenic records, including several gamma-emitting radionuclides varying in half-life from 5.6 day ^{52}Mn to 0.73 Ma ^{26}Al, tracks and rare gases have been carried out. The exposure age of the meteorite is estimated from cosmogenic components of rare gases to be 19.6 Ma. The track density varies by a factor of ~3 (from 4 to 12 × 10^6/cm^2) within the meteorite, indicating a preatmospheric body of ~9 cm radius (corresponding to a meteoroid mass of ~11 kg) and small ablation (1.5 to 3.6 cm). Trapped components in various rare gases are high and the solar component is present in the dark portion of the meteorite. Large excess of neutron-produced ^{82}Kr and ^{128}Xe in both the light and the dark lithology but very low ^{60}Co, indicating low neutron fluxes received by the meteoroid in the interplanetary space, are clear signatures of an additional irradiation on the parent body.

FALL OF THE METEORITE

On Tuesday, 2000 May 30, at ~1:45 P.M. a single stone weighing little <1 kg fell in the field of Jagdish Mali in Itawa Bhopji village (27°17' N, 75°72' E) of Chomu Tehsil, Jaipur District, Rajasthan, India. The fall was witnessed by a young lady, Phoolibai, who was watering her field situated ~50 m away. She described a whirling dust cloud accompanying a hissing sound with the fall of the meteorite. Due to sunny bright sky no meteor trail or fireball was seen. The meteorite was subsequently broken up in a few fragments (Fig. 1a), the main mass being ~660 g. The meteorite made a circular crater of ~40 cm in diameter and 20 cm deep (Fig. 1b) in the brownish soft soil of the field. Other witnesses indicated that the sound was heard over a distance of 3 to 4 km around the place of fall. Although the crater rim is nearly circular, the asymmetrical walls of the crater and distribution of ejecta suggest that the meteorite was travelling northwest to southeast, the direction being roughly from 34° west of north.

MICROSCOPIC AND PETROGRAPHIC EXAMINATION

The meteorite was roughly pear shaped and fully covered with thick fusion crust at the time of recovery (Fig. 1a). The fusion crust is dull black with a few striations and thumb impressions at the margins. The broken face shows several light coloured angular lithic fragments and abundant chondrules (≤2 mm in diameter) in a grey to dark grey matrix (Fig. 2a). Thin section studies show that minerals like olivine, orthopyroxene, troilite and numerous opaques are present. The abundance of olivines is high (60 to 70%) and pyroxenes occur in low abundance (15 to 20%). Feldspars are extremely rare. Numerous veins of troilite composition can be seen in thin sections. The boundaries of some chondrules are not much degraded (Figs. 2b and 3). Numerous irregular and planar fractures and angular nature of crystals of olivine (Fig. 2b) and adjoining ground mass show evidence of weak degree of shock and can be classified as S2 grade on the scale of Stöffler *et al.*

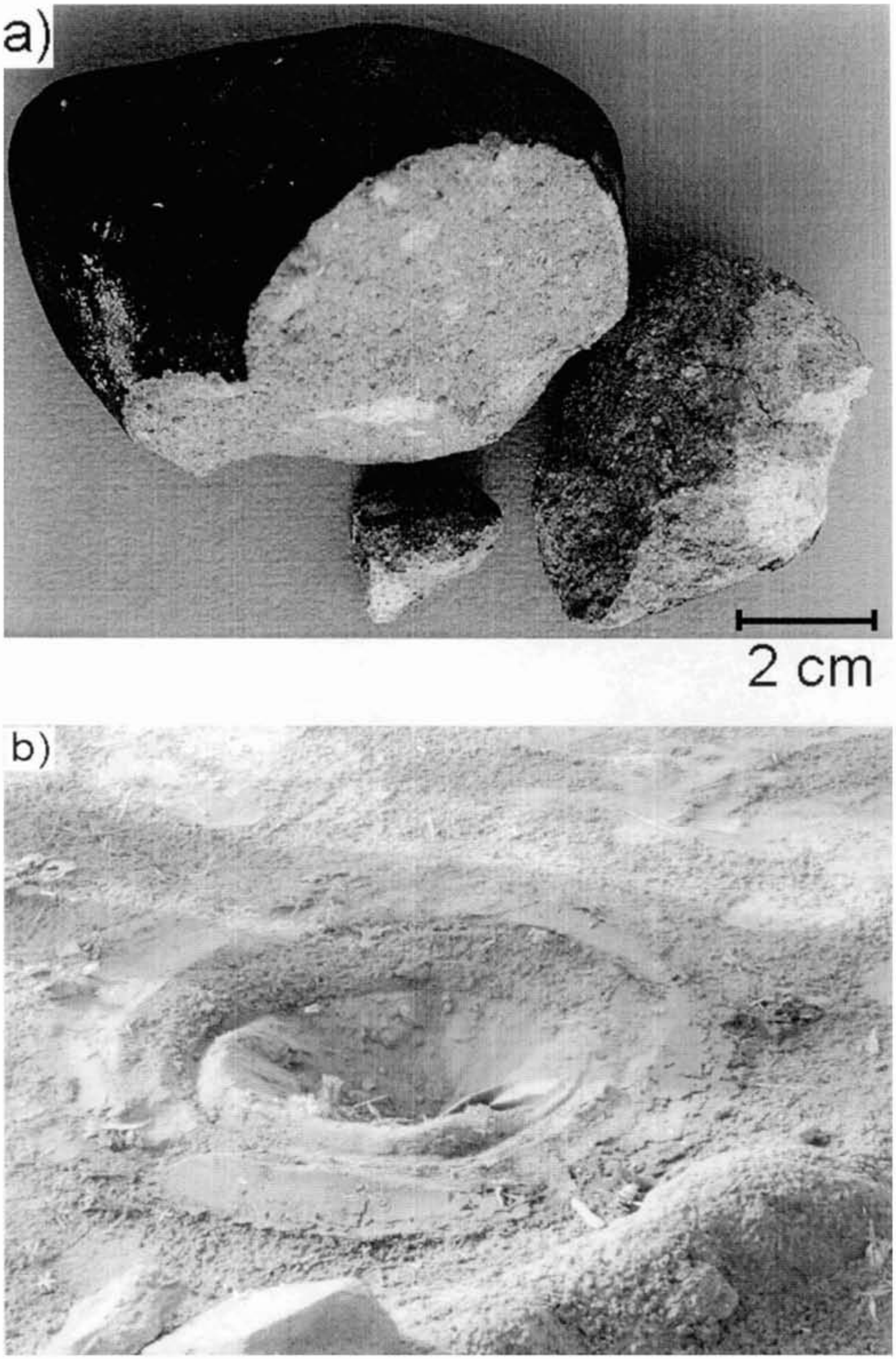

FIG. 1. (a) Photograph showing light angular lithic fragments in the dark matrix of the Itawa Bhopji meteorite. (b) Crater formed in the brown soil of the field due to impact of the meteorite. The circles were drawn on the soil to show the crater boundary. The conical crater having diameter ~40 cm is slightly asymmetrical.

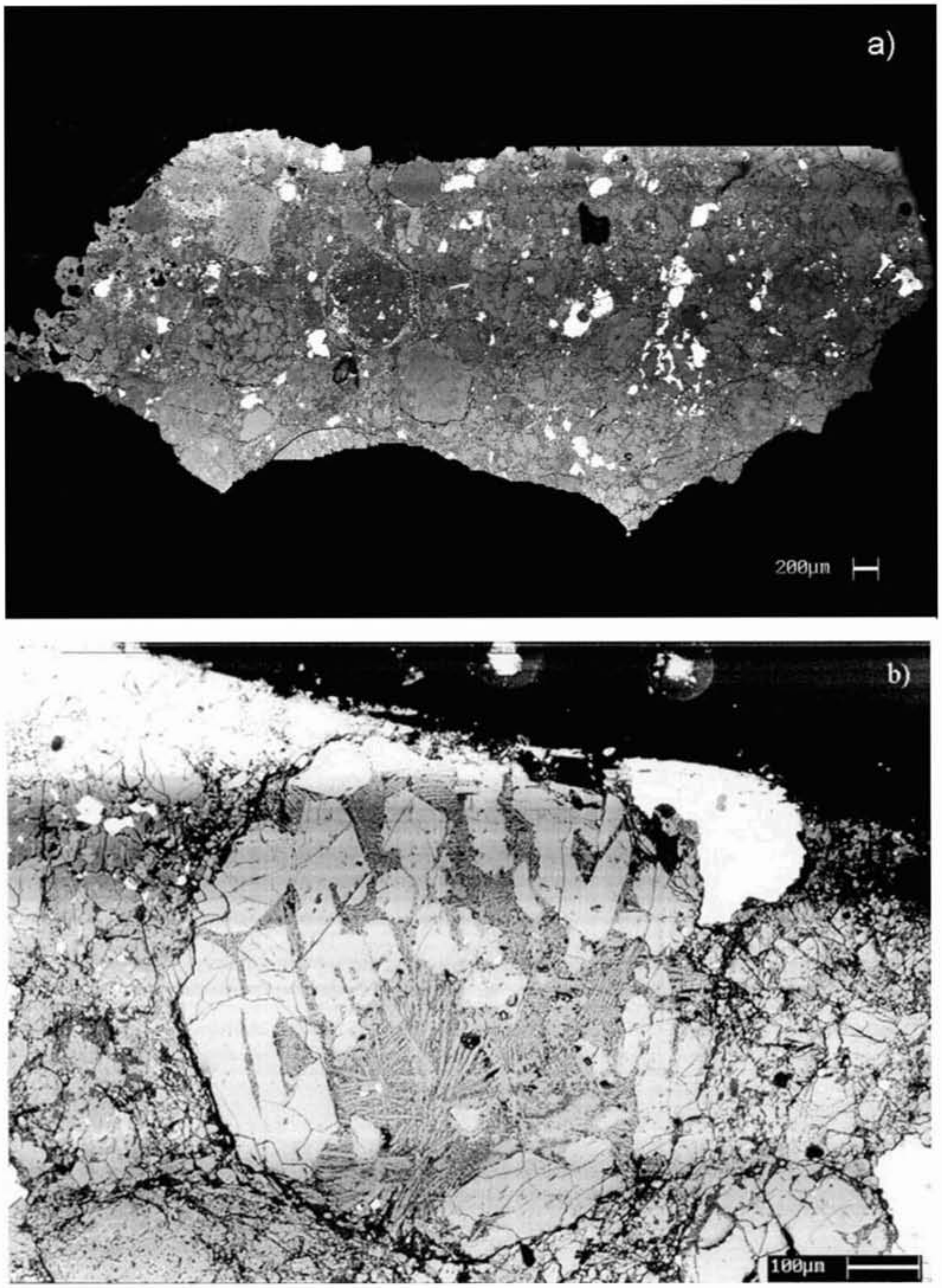

FIG. 2. (a) Backscatter electron images of the thick sections of Itawa Bhopji meteorite showing chondrules, metal and ilmenite veins; (b) enlarged view of a porphyritic olivine-pyroxene chondrule showing numerous fractures and angular grains in the ground mass.

(1991). All these evidences suggest that this meteorite is a regolith breccia. The chondrules are mostly granular and generally occur in size range of 0.1 to 1 mm, although some as small as 50 μm and as big as 2 mm are also present. Chondrules occur in a variety of textures (Figs. 3 and 4), for example, barred-olivine (BO), granular olivine (GO), porphyritic olivine (PO), porphyritic pyroxene (PP), porphyritic olivine-pyroxene (POP) and fine-grained pyroxene types (RP), the most common being porphyritic-olivine (PO). Within some chondrules, intergranular glass, which is turbid and partly devitrified, is occasionally present. Many chondrules have dark rims (Figs. 2 and 3). Presence of chondrules with slightly degraded

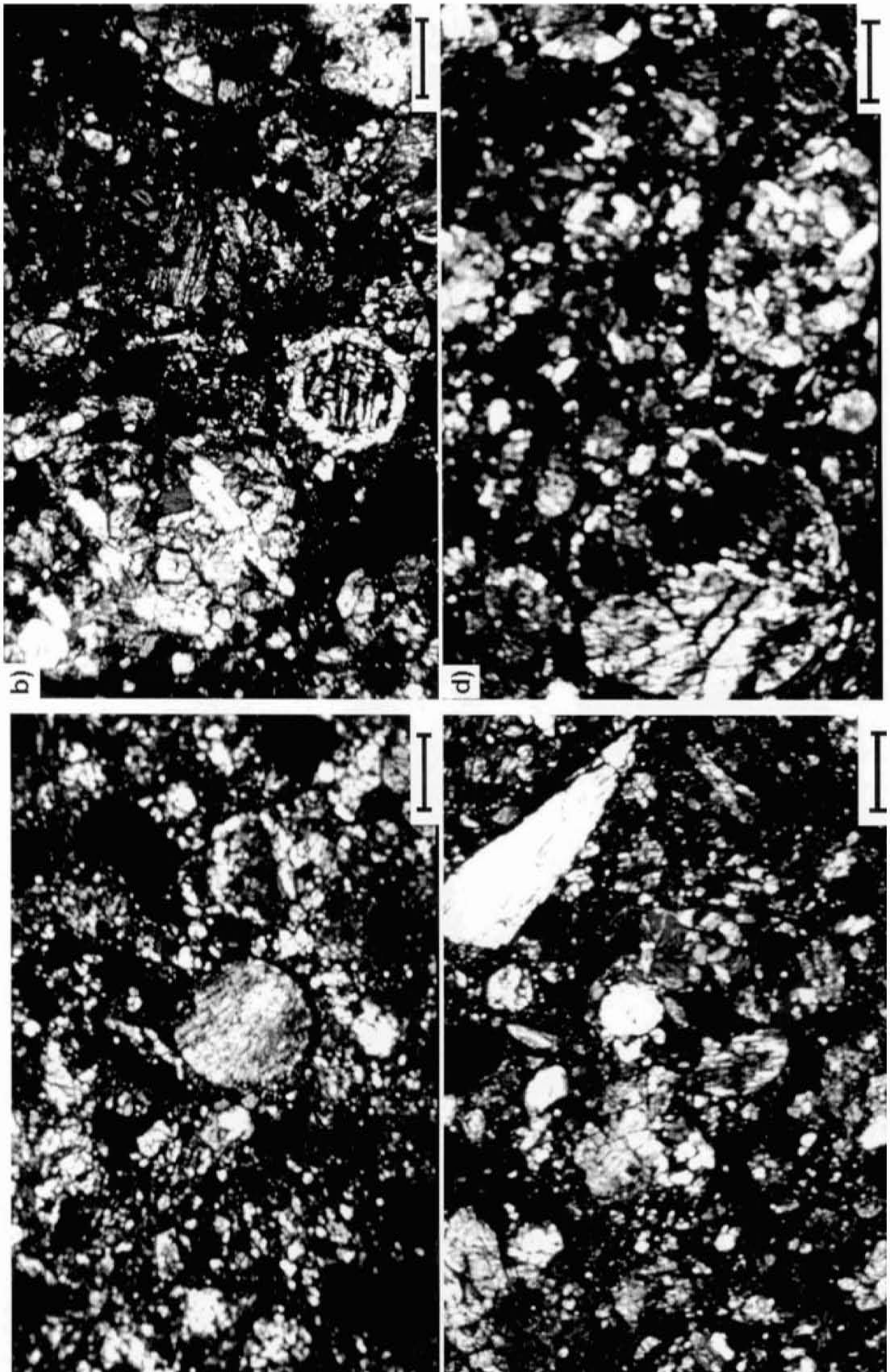

FIG. 3. Photomicrographs of thin section showing complete chondrules with sharp boundary (a) and (b) and degraded chondrules (c) and (d) indicating type 3-5 breccia components.

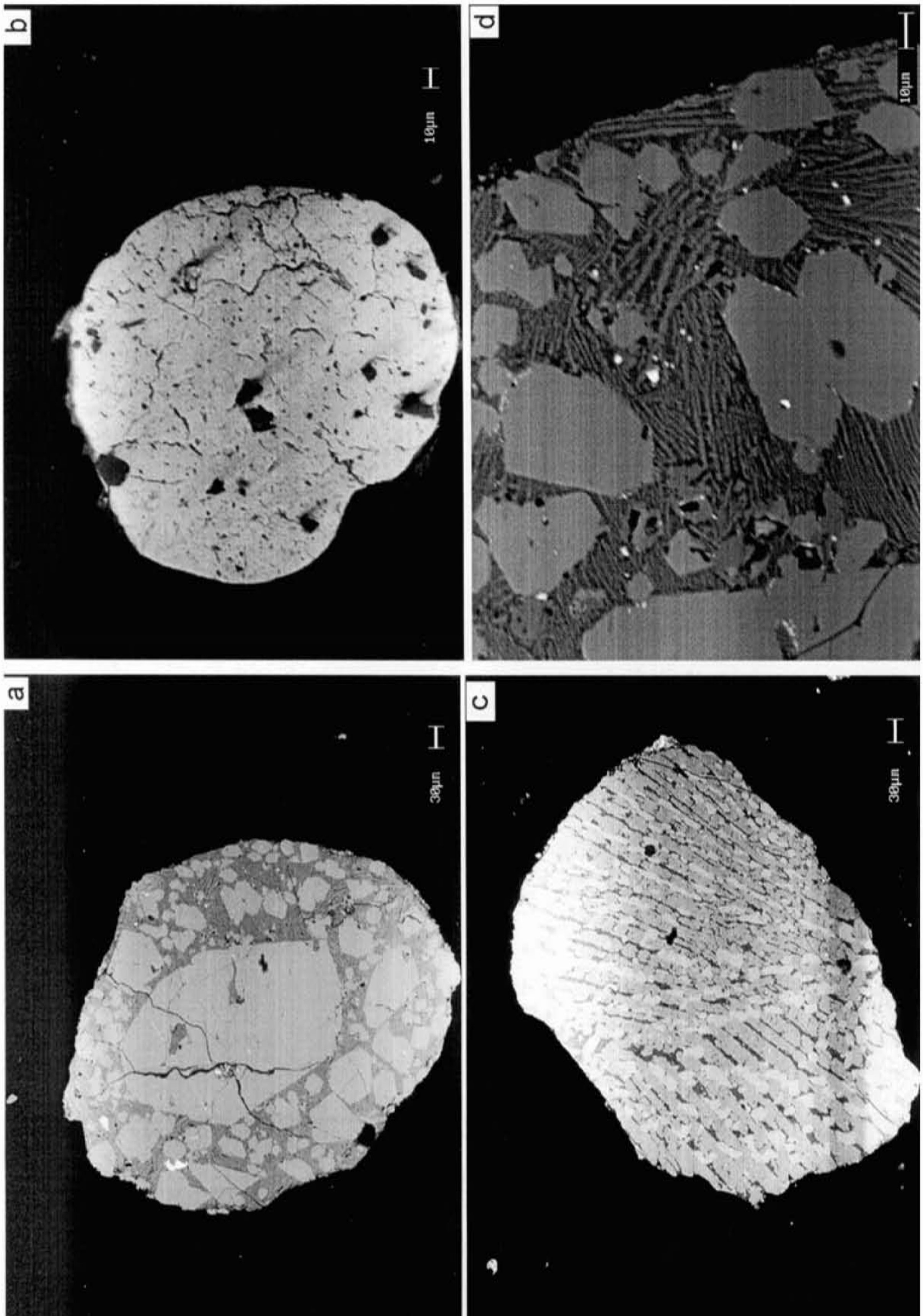

FIG. 4. Various types of chondrules: (a) porphyritic olivine with shock-induced cracks and fractures; (b) a round object with numerous opaques; (c) a barred degraded chondrule; (d) enlarged view of euhedral olivine chondrule with crystallites of pyroxene and minor opaques.

boundaries (Figs. 2 and 3) along with evidences of metal-silicate segregation and devitrified glasses inside the chondrules suggest higher metamorphic grade (*i.e.*, type 5). All these observations suggest that Itawa Bhopji is a mixture of clasts of petrologic types 3 to 5 (Van Schmus and Wood, 1967). Mineral chemical analyses of olivines (Fa_{24-26}) and pyroxenes (Fs_{20-22}) within the equilibrated lithologies (light clasts), given in Table 1, indicate that the meteorite belongs to the L group of ordinary chondrites. Olivine (Fa_{5-29}) and low calcium pyroxene (Fs_{5-37}) within the unequilibrated components are highly variable indicating that the stone contains clasts of petrological grades 3 to 5.

CHEMICAL ANALYSIS

Elemental concentrations were determined for the bulk meteorite (dark matrix) as well as for the light and dark lithologies using inductively-coupled plasma atomic emission spectrophotometry (ICP-AES)/atomic absorption spectrophotometry (AAS) and instrumental neutron activation analysis (INAA). Clean fragments (2 to 2.5 g) from both the lithologies were crushed and powdered separately in an agate mortar. While crushing the light and dark lithologies some metal particles (samples ML and MD, respectively) could not be crushed into fine powder. Although the metal separation is not quantitative, we have analyzed these fractions separately to determine the composition of the metal. Light clasts were found to contain more metal (3.4%) compared to the dark matrix (0.6%). About 300 mg each of light and dark powders were dissolved in HF-HCl for ICP-AES/AAS analysis. Dhajala (H3.8) meteorite and diabase W-2 were used as standards. INAA was carried out in two separate irradiations. In the first batch of samples, four aliquots (40 to 60 mg) of the bulk meteorite were analyzed while the second batch consisted of four aliquots (~50 mg) each from light and dark powders and their metal separates (ML and MD) and an aliquot of the bulk sample. These samples together with standards (Allende (CV3), Dhajala (H3.8), BCR-1 and AGV-1) were irradiated in Dhruva reactor of Bhabha Atomic Research Center, Mumbai. The irradiated samples were counted at different intervals of time on a high-purity Ge detector (148 cm^3) located in 10 cm thick lead shield following standard procedures (Laul, 1979; Shukla *et al.*, 1997). In this way concentrations of Al, Mg, Ca, Ti, Mn, Fe, Ni, Na and K were determined using ICP-AES/AAS and elements such as Fe, Ni, Co, Cr, Na, K, Zn, Sc, La, Ce, Sm, Eu, Yb, Ir, Os and Au were determined using INAA procedures. The weighted mean concentrations, representing the bulk meteorite, are given in Table 2 where concentrations of the light and dark lithology are also included. As expected, the concentrations of siderophile elements were found to be very high in metal separates ML and MD. The composition of ML is determined to be: Fe (80.8%), Ni (6.55%), Co (7419 ppm), Cr (766 ppm), Ir (1.7 ppm), Os (1.64 ppm), Au (1.03 ppm), Na (641 ppm) and Sc (0.53 ppm) and of MD: Fe (83.7%), Ni (9.97%), Co (5965 ppm), Cr (192 ppm), Ir (3.4 ppm), Os (2.06 ppm), Au (1.34 ppm), Na (411 ppm) and Sc (0.23 ppm), respectively. Based on Na and Sc concentrations, we infer that the metal separation was not pure and 6 to 8% of silicate in ML and 3 to 6% in MD was still present. While computing the average elemental concentrations for light and dark fractions, given in Table 2, appropriately weighted contribution from the metallic fractions were taken into account. The concentrations of various elements do not show any significant difference between the bulk, light and dark lithologies indicating that they are compositionally similar. The values for siderophile elements including platinum group elements (PGE) (Fe, Co, Ni, Ir, Os and Au) match well with those of L class of ordinary chondrites (Kallemeyn *et al.*, 1989).

MD shows higher concentration of Ni, Ir and Os as compared to ML, whereas Co shows an opposite trend. Here we discuss the ratios Ir/Ni and Au/Ni based on the work of Rambaldi (1976, 1977) and Kong and Ebihara (1997). The Ir/Ni ratios in ML and MD are 2.6×10^{-5} and 3.4×10^{-5}, respectively which lie in the range observed in metal from L chondrites (Ir/Ni = $(2.4–3.8) \times 10^{-5}$). Similarly Au/Ni ratio of 1.6×10^{-5} for ML and 1.3×10^{-5} for MD are close to the values observed for metals in L chondrites (Au/Ni = $(1.1–1.5) \times 10^{-5}$). Ir concentration in MD is about a factor of 2 higher than in ML and, as mentioned above, the Ir/Ni is also higher in MD compared to ML, indicating a higher fraction of fine-grained metallic component in MD compared to ML. This fine-grained metallic component has been suggested to be plessite (Rambaldi, 1977) and Ir as well as Os has higher affinity for

TABLE 1. Composition (wt%) of representative olivines and pyroxenes within the Itawa Bhopji (L3-5) ordinary chondrite.

	Pyroxene				Olivine				
MgO	35.8	34.4	21.7	29.0	38.4	37.7	47.2	35.0	38.6
Al_2O_3	0.16	0.76	<0.04	0.13	<0.06	–	–	–	<0.07
SiO_2	58.9	58.2	53.5	55.4	38.5	37.7	40.4	37.8	38.2
CaO	0.27	0.62	0.69	0.54	<0.04	–	0.21	–	–
TiO_2	<0.05	<0.05	<0.05	0.11	<0.05	–	<0.10	–	–
Cr_2O_3	0.53	0.34	0.38	0.45	<0.05	<0.11	–	0.23	–
MnO	0.21	0.30	0.61	0.25	0.48	<0.12	0.53	0.22	0.55
FeO	3.7	5.0	22.5	13.2	22.3	23.9	10.9	25.3	21.9
Fs/Fa	5.5	7.4	36.4	20.1	24.6	26.3	11.5	28.9	24.1

TABLE 2. Chemical composition of the Itawa Bhopji L3-5 chondrite.*

Element	Concentration		
	Bulk	Light	Dark
Al (%)	1.23	1.26	1.2
Ca (%)	1.3	1.38	1.40
Mg (%)	15.45	15.5	15.4
Fe (%)	21.6	21.37	21.27
Ni (%)	1.21	1.18	1.11
Co (ppm)	600	577	537
Cr (ppm)	3862	3856	3765
Na (ppm)	7404	7680	N.M.
K (ppm)	824	N.M.	N.M.
Zn (ppm)	44	53	39
Se (ppm)	8.3	7.5	9.0
Mn (ppm)	2425	2440	2409
Ti (ppm)	607	603	611
Sc (ppm)	8.40	8.5	8.2
La (ppm)	0.35	N.M.	N.M.
Ce (ppm)	1.35	1.27	1.53
Sm (ppm)	0.21	0.20	0.21
Eu (ppm)	0.09	0.09	0.08
Yb (ppm)	0.23	N.M.	N.M.
Ir (ppb)	512	521	486
Os (ppb)	458	464	405
Au (ppb)	157	157	148

*Errors for major elements are $\leq$2% except for Ca (5%). For trace elements errors are $\leq$10% and represent 1σ statistical counting errors for elements determined by INAA, except for Os where the maximum error is 17%. Abbreviations: N.M = not measured.

this phase. Detailed studies of metals from various groups of chondrites have shown that the siderophile elements have different affinity for kamacite and taenite phases. Cobalt, for example, has higher affinity for kamacite whereas Ni, Ir, Os and Au have higher affinity for taenite and fine-grained metallic components. Therefore, different ratios in MD and ML could be due to different proportions of kamacite and taenite and their grain sizes in these two phases. Higher Ni, Ir and Os content in MD is consistent with its higher proportion of taenite.

Based on the bulk chemical composition (Fe, Ni, Co, Ir, Os and Au) the meteorite is classified as an L chondrite (Kallemeyn *et al.*, 1989). Mössbauer spectroscopy of the meteorite, although consistent with this classification, has revealed that it is relatively more oxidised with unusually high olivine to pyroxene ratio (H. C. Verma and R. P. Tripathi, pers. comm., 2001), consistent with the petrographic observations.

COSMOGENIC RECORDS

Cosmic-Ray Tracks

Cosmic-ray tracks, radionuclides and rare gases have been measured in this meteorite. Track density was measured in several samples (taken 1–3 mm below the crusted surface, marked "s" in Table 3) and in interior samples (marked "i"). Two orthogonal profiles across the broken faces of the meteorite were also studied. The sample locations are shown in Fig. 5. A small piece collected from Samod Police Station (C-7) was also analyzed. Samples CCD and CCL represent the dark and light material which were used for rare gas analyses. The tracks were measured after appropriate etching of olivines in WN solution (40% EDTA + 1% oxalic acid and orthophosphoric acid, made to pH 8.0 by adding NaOH; Krishnaswami *et al.*, 1971) for 5 h following the procedure described by Bhandari *et al.* (1980). The track density (Table 3) was found to vary between 4.1×10^6 to $1.2 \times 10^7/\text{cm}^2$ showing small but measurable gradient across the meteorite. The center of the meteoroid should have been located close to the sample #11 since it has the maximum shielding. Track production rates within the meteorite were calculated using the exposure age of 19.6 Ma, estimated from the concentration of cosmogenic components in rare gases as discussed later. Shielding depths for each sample were calculated by comparing these values with the track production rates given by Bhattacharya *et al.* (1973), after appropriate corrections for the low track recording sensitivity of olivines (factor of 2) was applied to the track density (Bhandari *et al.*, 1972). The results (Table 3) show that the shielding depths are small, ranging between 1.5 and 3.6 cm suggesting roughly symmetric all round ablation of the meteoroid. The least ablated part of the meteorite is the apex (Fig. 5). The meteorite, thus, belongs to the ablation class I of Bhandari *et al.* (1980). The data yield the preatmospheric size

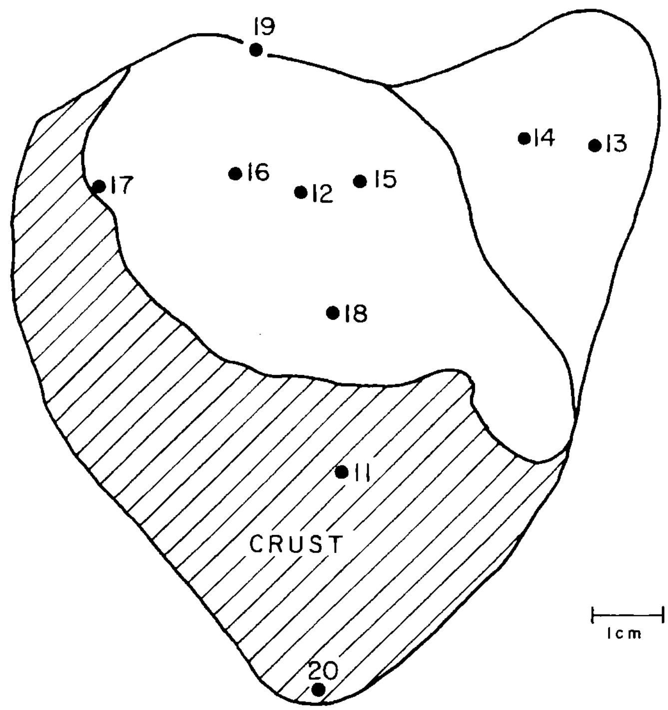

FIG. 5. Locations of samples studied for particle tracks (see Table 3).

TABLE 3. Track density in the Itawa Bhopji meteorite.

Sample*	Track density per cm^2 (number of tracks)	Track production rate per cm^2 Ma†	Mean shielding depth (cm)
11s	4.44×10^6 (320)	4.53×10^5	3.6
12s	6.71×10^6 (1453)	6.8×10^5	2.5
13s	4.74×10^6 (482)	4.84×10^5	3.5
14i	6.94×10^6 (1468)	7.1×10^5	2.3
15i	6.46×10^6 (995)	6.6×10^5	2.5
16i	4.65×10^6 (320)	4.75×10^5	3.5
17s	8.8×10^6 (603)	9.0×10^5	1.7
18i	5.08×10^6 (783)	5.2×10^5	3.1
19s	5.16×10^6 (601)	5.26×10^5	3.1
20s	1.23×10^7 (1134)	1.25×10^6	1.5
C-III (random)	4.1×10^6 (552)	4.1×10^5	3.7
C-7 (Samod)	9.23×10^6 (1014)	9.44×10^5	1.9
CCD (dark)	7.36×10^6 (1182)	7.5×10^5	2.5
CCL (light)	9.0×10^6 (1017)	9.2×10^5	1.8

*"s" represents near-surface and "i" represents interior sample.
†Based on exposure age of 19.6 Ma and corrected for lower track recording efficiency of olivines.

of the meteoroid (~9 cm radius) corresponding to ~11 kg. This implies that the meteoroid suffered an ablation of about 92 ± 2%. If we use the calculations of Potdar (1981) which relates mass ablation to entry velocity of meteoroid for various angles of entry, a geocentric velocity of ~19 km/s is estimated for the Itawa Bhopji meteoroid. Since this meteorite has light and dark clasts, typical of gas-track-rich meteorites, we looked for irradiated grains containing track density gradients or extremely high densities. Absence of such grains indicate that the exposure on the surface of the parent body was brief.

Cosmogenic Radionuclides

The main fragment weighing ~660 g was available within a week of fall for non-destructive counting permitting measurement of several short-lived radionuclides, such as 5.6 day ^{52}Mn. In all, 12 gamma-emitting radionuclides (^{7}Be, ^{22}Na, ^{26}Al, ^{46}Sc, ^{48}V, ^{51}Cr, ^{52}Mn, ^{54}Mn, ^{56}Co, ^{57}Co, ^{58}Co and ^{60}Co) were measured in the meteorite using a large volume (~400 cm^3), low-background, high-purity germanium gamma-ray spectrometer located in a 20 cm thick lead shield, described in Shukla *et al.* (2001). ^{40}K (K = 824 ppm; Table 2) has been used as an internal standard for estimating the activity levels of the cosmogenic radionuclides following the procedure of Bhandari *et al.* (1989). Four sets of counting, each for about a week, between 2000 June 7 and July 7 were made to resolve the short- and long-lived radionuclides. For the long-lived radionuclides, the mean counting rates, averaged over all the sets have been used whereas for the short-lived radionuclides only set I or/and II have been used. The measured counting rates as well as the calculated activities are given in Table 4. We note that the activity of the neutron-capture isotope, ^{60}Co (≤0.48 dpm/kg), was too low to be measured accurately. On comparing it with the calculated production rates given by Spergel *et al.* (1986), for cobalt concentration of 600 μg/g (Table 2), we find that the observed activity of ^{60}Co indicates extremely low thermal neutron fluxes which, in turn, implies low shielding depth and small preatmospheric size (≤10 cm) of the meteoroid in the interplanetary space. This is consistent with the track data discussed above. Similarly, the observed ^{26}Al activity (40.2 ± 0.5 dpm/kg) falls in the range of the production depth profile of ^{26}Al for a spherical meteoroid of ~9 cm radius (Bhandari *et al.*, 1993; Leya *et al.*, 2000), consistent with the track and ^{60}Co data. In this way we find that the track, ^{26}Al and ^{60}Co data are mutually consistent with a preatmospheric size of ~9 cm and small ablation of the meteoroid. In Table 4, we compare the observed activities with those observed in the Torino (H6) meteorite because that is the only other recent fall in which all these radionuclides have been measured. Significant differences in the activities of some radioisotopes in the two meteorites are obvious from Table 4. There are several reasons for these differences:

(1) Target element composition: Torino is an H chondrite whereas Itawa Bhopji belongs to the L group. Because of the low Fe concentration (21.6%) the radionuclides, which are produced in iron target of the meteorite, are expected to be ~17% lower in Itawa Bhopji compared to Torino (Fe = 26.1%).

(2) Phase of the solar cycle: the Torino meteorite fell after the solar minimum, when the galactic cosmic-ray intensity was at a maximum whereas Itawa Bhopji fell just after the solar maximum of solar cycle 23. Low activities of short-lived nuclides having half-life of a few years or smaller would be expected in Itawa Bhopji due to stronger modulation of the galactic cosmic-rays because of higher heliomagnetic field at solar maximum.

TABLE 4. Cosmogenic radionuclides* in the Itawa Bhopji meteorite.

Radio-nuclide	Half-life	γ-Energy (keV)	Efficiency (%)	Itawa Bhopji (L3–5) Solar maximum 2000 May 30		Torino† (H6) Solar minimum 1988 May 18 Activity (dpm/kg)	Activity ratio Itawa Bhopji/ Torino
				Counting rate	Activity (dpm/kg)		
^{52}Mn	5.6 days	1434.3	3.5	0.12 ± 0.02	9.4 ± 1.6	20.3 ± 1.8	0.46
^{48}V	16 days	983.5	4.65	0.088 ± 0.005	4.6 ± 0.3	20.8 ± 1.5	0.27
		1311.6	3.5	0.078 ± 0.005	5.8 ± 0.06	–	–
^{51}Cr	27.7 days	320.07	7.0	0.072 ± 0.01	27.9 ± 4	76 ± 7	0.37
^{7}Be	53.3 days	477.56	6.4	0.074 ± 0.05	31.2 ± 2	59 ± 6	0.52
^{58}Co	70.78 days	810.75	5.1	0.0195 ± 0.003	1.1 ± 0.15	11 ± 0.7	0.1
^{56}Co	78.8 days	846.75	5.14	0.051 ± 0.003	2.8 ± 0.016	7.7 ± 0.75	0.36
^{46}Sc	83.9 days	889.26	4.85	0.052 ± 0.003	2.9 ± 0.017	10.4 ± 2	0.28
^{57}Co	271.35 days	122.07	8.2	0.067 ± 0.003	2.6 ± 0.04	16.3 ± 1	0.16
^{54}Mn	312.2 days	834.8	5.05	0.055 ± 0.004	29.7 ± 0.3	121 ± 2	0.25
^{60}Co	5.27 years	1173.20	3.65	0.0067	≤0.49	2.8 ± 0.3	–
		1332.51	3.5	0.0060	≤0.47	–	–
^{22}Na	2.6 years	1274.54	3.5	0.055 ± 0.004	44 ± 0.4	80 ± 1	0.55
^{26}Al	0.73 Ma	1808.6	2.45	0.036 ± 0.003	40.2 ± 0.4	54 ± 1.1	0.74
^{40}K	–	–	–	2.065 ± 0.009	–	–	–
^{22}Na/^{26}Al	–	–	–	–	1.1	1.48	–

*The activity is calculated at the time of fall.
†Bhandari *et al.* (1989).

(3) Size of the meteorite: Torino meteoroid was a body with ~20 cm radius and the nuclear cascade due to interaction with galactic cosmic rays is developed to a significant extent whereas Itawa Bhopji was a small meteoroid (~9 cm radius) in which the nuclear cascade would not have developed fully. Neutron-capture effects in small bodies are therefore very small. In fact, for such a small ablation (~1 cm), solar proton effects become significant, although their contribution in whole body counting will be only marginally observable.

The activity ratio of isotope pairs having comparable half-life (*e.g.*, ^{57}Co/^{54}Mn or ^{48}V/^{51}Cr) are similar in Itawa Bhopji and Torino within ±20% (Table 4) as would be expected from calculations of their production rates. On the other hand, high ^{56}Co activity relative to ^{57}Co or ^{58}Co (Table 4) suggests that some contribution from solar protons due to ^{56}Fe (p,n) ^{56}Co reaction in Itawa Bhopji may be present. The ^{22}Na/^{26}Al ratio in Itawa Bhopji is 1.1. This is a measure of the integrated fluxes of cosmic rays over a few years (one or two mean lives of ^{22}Na) prior to the fall of the meteorites. Itawa Bhopji fell just after the solar maximum of solar cycle 23. About 35 chondrites have been studied for ^{22}Na/^{26}Al (Bhandari *et al.*, 1994; Bonino and Cini Castagnoli, 1997; Murty *et al.*, 1998). In Fig. 6, we show the calculated variation in ^{22}Na/^{26}Al based on Climax neutron monitor data (Solar Geophysical Data, 2000), following the procedure of Bhandari *et al.* (1989) for H, L and LL group of meteorites. The difference between the two curves (H and L or LL) is due to chemical abundance of target elements. Averaged over a solar cycle, the galactic cosmic-ray produced ^{22}Na/^{26}Al = 1.5 in H and 1.35 in L and LL, and it is largely independent of the size of the meteoroid. This ratio also varies roughly in anticorrelation with sun spot numbers with a small phase difference, determined by the half-life of ^{22}Na. With a few exceptions, most of the chondrites have ratio close to the expected value. Ratios higher than the expected values can arise due to a number of reasons: (1) short exposure age or fragmentation in interplanetary space shortly before the fall of the meteorite (within 2 Ma or so, until ^{26}Al does not attain secular equilibrium with its production), as observed in the case of Jilin H meteorite (Heusser *et al.*, 1985); or (2) cosmic-ray gradient within the heliosphere, as in the case of Dhajala, which had high orbital inclination (Bhandari *et al.*, 1978). There are some other meteorites which show marginal discrepancy and these are probably due to spatial variation of cosmic-ray fluxes within the heliosphere or their peculiar exposure history. In the case of meteoroids with small ablation (<1 cm), the solar production of ^{26}Al due to the reactions ^{26}Mg (p,n) ^{26}Al and ^{25}Mg (p,γ) ^{26}Al become significant leading to low ^{22}Na/^{26}Al. This may partly explain the low ^{22}Na/^{26}Al ratio in Itawa Bhopji since the ablation on some faces is 1–2 cm (Table 3). A recent analysis of the *aa* index has shown that the solar magnetic field has doubled during the past 100 years and increased by a factor of 1.3 since 1964 (Lockwood *et al.*, 1999; Solanki *et al.*, 2000), leading to reduction in galactic cosmic-ray fluxes in the heliosphere. Analysis of neutron monitor count rates since the data are available (1953) has not been made to estimate any change in heliomagnetic field although this has

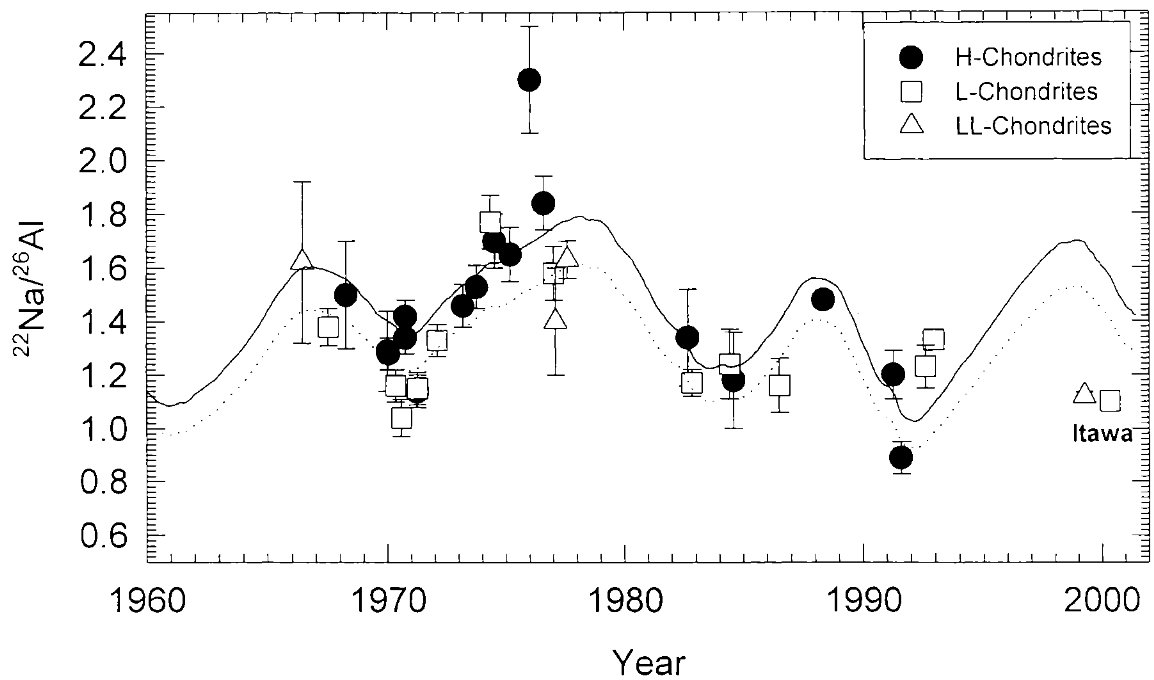

FIG. 6. $^{22}Na/^{26}Al$ observed in chondrite falls since 1966 compared with the values calculated from Climax neutron monitor count rates shown by continuous and dotted curves for H, L and LL group of meteorites, respectively. For source of data see Evans *et al.* (1982); Bhandari *et al.* (1994); Bonino and Castagnoli (1997). Itawa Bhopji seems to have an anomalous low value (1.1) as compared to the expected value of 1.4.

been confirmed by ^{44}Ti measurements in meteorites that fell during the past two centuries (Bonino *et al.*, 2001a). The $^{22}Na/^{26}Al$ value, ~20% lower than the expected value of 1.4 may partly be due to these changes in the galactic cosmic-ray fluxes with time. It may be noted that a low ratio of $^{22}Na/^{26}Al$ has also been found in another meteorite Sabrum (LL6) which fell shortly before Itawa Bhopji (Ghosh *et al.*, 2002).

Noble Gas Studies

Itawa Bhopji has light clasts embedded in a dark matrix, typical of gas-rich meteorites. We have analyzed a sample from each of these two lithologies (CCL and CCD) from adjacent locations, taken from interior of the meteorite to look for the possible presence of solar gases in addition to the cosmogenic components. Track densities in these two samples were also measured to obtain their cosmic-ray shielding depth, which is determined to be 1.8 and 2.5 cm, respectively (Table 3). The samples were wrapped in Al-foil, loaded into the extraction system of the noble gas mass spectrometer and analyzed for nitrogen and all the noble gases using standard procedures (Murty *et al.*, 1998). Here, we discuss the light noble gases data; nitrogen results will be reported elsewhere. Gases extracted by stepwise heating were analyzed for their isotopic composition. The data reported in Table 5 have been corrected for blanks, interferences and instrumental mass discrimination as described in earlier publications (Murty *et al.*, 1998; Bhandari *et al.*, 1998; Bonino *et al.*, 2001b).

The dark lithology has about an order of magnitude higher ^{22}Ne and ^{36}Ar as compared to the light lithology. Also the $^{20}Ne/^{22}Ne$ ratios in the dark sample are significantly higher, indicative of the presence of the solar component. The noble gas isotopes reveal a complex irradiation record as discussed below.

Cosmic-Ray Exposure Ages

He, Ne and Ar are mostly dominated by cosmogenic and radiogenic (^{4}He and ^{40}Ar) components. Small amounts of trapped Ne and Ar (and probably ^{4}He) are also present. The cosmogenic components were estimated using standard procedures and are given in Table 6. Ne in the light lithology is almost purely cosmogenic with $(^{22}Ne/^{21}Ne)_c$ = 1.24, indicating shallow depth of irradiation (~1 cm) within the meteoroid, consistent with the track density data. If we calculate the production rates corresponding to this shielding depth, and the measured chemical composition (see Table 2) for ^{3}He, ^{21}Ne (Eugster, 1988), and ^{38}Ar (Marti and Graf, 1992) we get exposure ages (in Ma) of T_{21} = 17.3, T_3 = 11.9 and T_{38} = 14.1. Assuming identical shielding of light and dark lithologies to cosmic rays, since both were located adjacent to each other within the meteorite, we take the same $(^{22}Ne/^{21}Ne)_c$ for the dark lithology (1.24). Two additional observations further justify this choice. In the Ne three-isotope plot, the best-fit line for the dark sample data passes through the light sample data that are purely cosmogenic. Also, for the 1700 °C step of

TABLE 5. He, Ne and Ar in the light and dark lithologies of Itawa Bhopji meteorite*.

Temp. (°C)	^{4}He (10^{-8} ccSTP/g)	^{22}Ne (10^{-8} ccSTP/g)	^{36}Ar (10^{-8} ccSTP/g)	^{3}He/^{4}He	^{20}Ne/^{22}Ne	^{21}Ne/^{22}Ne	^{38}Ar/^{36}Ar	^{40}Ar/^{36}Ar
Light lithology (209.785 mg)								
400	136.4	0.029	0.031	0.0080 ± 0.0007	1.484 ± 0.029	0.7979 ± 0.0243	0.2339 ± 0.0005	2983 ± 33
1000	1535	1.93	0.117	0.0102 ± 0.0009	0.8156 ± 0.0018	0.7942 ± 0.0008	1.058 ± 0.001	8884 ± 87
1700	60.8	2.60	0.957	0.0266 ± 0.0022	0.9640 ± 0.0048	0.8079 ± 0.0008	0.5159 ± 0.0002	470.7 ± 4.6
Total	1732	4.56	1.10	0.0107 ± 0.0009	0.9046 ± 0.0037	0.8020 ± 0.0009	0.5653 ± 0.0003	1433 ± 14
Dark lithology (362.831 mg)								
400	793.7	0.298	0.870	0.0040 ± 0.0003	9.449 ± 0.001	0.2172 ± 0.0002	0.1923 ± 0.0001	722.3 ± 7.3
800	1758	9.91	3.846	0.0060 ± 0.0005	11.14 ± 0.03	0.1470 ± 0.0005	0.1975 ± 0.0001	358.8 ± 3.6
1000	257.3	19.50	7.765	0.0074 ± 0.0006	11.95 ± 0.04	0.0853 ± 0.0001	0.1902 ± 0.0001	63.81 ± 0.64
1200	60.7	5.90	6.861	0.0063 ± 0.0005	10.22 ± 0.03	0.1614 ± 0.0001	0.1953 ± 0.0003	104.8 ± 1.0
1700	20.4	4.21	11.92	0.0128 ± 0.0011	7.196 ± 0.010	0.3733 ± 0.0003	0.2004 ± 0.0001	58.20 ± 0.60
Total	2890	39.82	31.27	0.0056 ± 0.0005	10.97 ± 0.03	0.1434 ± 0.0002	0.1961 ± 0.0001	125.3 ± 1.3

* Errors in concentrations are ±10%. Errors in isotopic composition represent 95% confidence limits.

TABLE 6. Cosmogenic components and exposure ages.

Sample	Cosmogenic (10^{-8} ccSTP/g)			Exposure age (Ma)		
	^{3}He	^{21}Ne	^{38}Ar	T_3	T_{21}	T_{38}
Light	18.5	3.63	0.474	11.9	17.3	14.1
Dark	16.3	4.59	0.289	10.6	21.9	8.6

the dark sample, wherein the cosmogenic contribution is maximum, the $(^{22}Ne/^{21}Ne)_c$ is calculated to be 1.27, very close to the value of 1.24 observed for the light sample. For this shielding parameter and the measured chemical composition (see Table 2) we have calculated the production rates, as we did for the light sample and derived the following cosmic-ray exposure ages for the dark lithology: T_3 = 10.6 Ma; T_{21} = 21.9 Ma; and T_{38} = 8.6 Ma. The exposure ages T_3 (11.9 and 10.6 Ma for the light (L) and dark (D), respectively) are consistent with each other within uncertainties of measurement. While T_{21}(L) = 17.3 Ma is lower than T_{21}(D) = 21.9 Ma, T_{38}(L) = 14.1 is higher than T_{38}(D) = 8.6 Ma. In view of the fact that the shielding conditions and chemical composition are similar for both the light and dark lithology samples, the discrepancies among the cosmic-ray exposure ages for the light and dark lithologies based on various rare gas isotopes are likely to be a reflection of any (or a combination) of the following reasons: (1) partial gas loss; (2) inappropriate production rate calculation; and (3) multiple irradiation of Itawa Bhopji; a space irradiation and a parent body irradiation, as happened in the case of Fayetteville (Wieler *et al.*, 1989) and Monahans meteorites (Bogard *et al.*, 2001). Though the absolute cosmic-ray exposure ages might depend on the method adopted for calculating the production rates (*e.g.*, Wieler *et al.*, 1996; Leya *et al.*, 2000) the relative differences in cosmic-ray exposure ages for the two lithologies should remain the same. The low values of T_3 are a reflection of partial He loss. The low values of T_{38} on the other hand are due to the presence of the neutron-produced $^{36}Ar_n$ from ^{35}Cl (n,γ) reaction, which results in an underestimate of $^{38}Ar_c$ and an apparent lower T_{38} (Wieler *et al.*, 1996; Bogard *et al.*, 1995). The amount of $^{36}Ar_n$ is expected to be larger in the dark sample compared to the light, as indicated by the higher ^{129}Xe in the dark sample (see Table 7), resulting in an apparently much lower value of T_{38}(D) as compared to T_{38}(L). The 26% difference between T_{21} of light and dark samples (17.3 and 21.9 Ma, respectively) can probably be interpreted as an additional irradiation for the dark lithology under different shielding conditions, although this seems unlikely, since the shielding parameter $(^{22}Ne/^{21}Ne)_c$ for both L and D is similar. Considering 10% uncertainty in the measurements of the concentration and an additional 5 to 10% uncertainty in the estimates of production rate, T_{21}(L) and T_{21}(D) seem to overlap within errors. We therefore take their average of 19.6 Ma as the exposure age of Itawa Bhopji. The 19.6 Ma exposure age obtained from ^{21}Ne represents the recent space exposure of the Itawa Bhopji meteoroid, as a 9 cm radius object.

TABLE 7. Trapped and radiogenic components (in ccSTP/g units) for Itawa Bhopji samples.

Sample	^{4}He	^{20}Ne	^{36}Ar	^{40}Ar$_r$	^{84}Kr	^{132}Xe	^{129}Xe$_r$
	10^{-8} ccSTP/g				10^{-10} ccSTP/g		
Light	840	0.9	0.80	1576	1.1	2.3	0.9
Dark	2010	432	31.1	3918	14.5	15.8	19.6

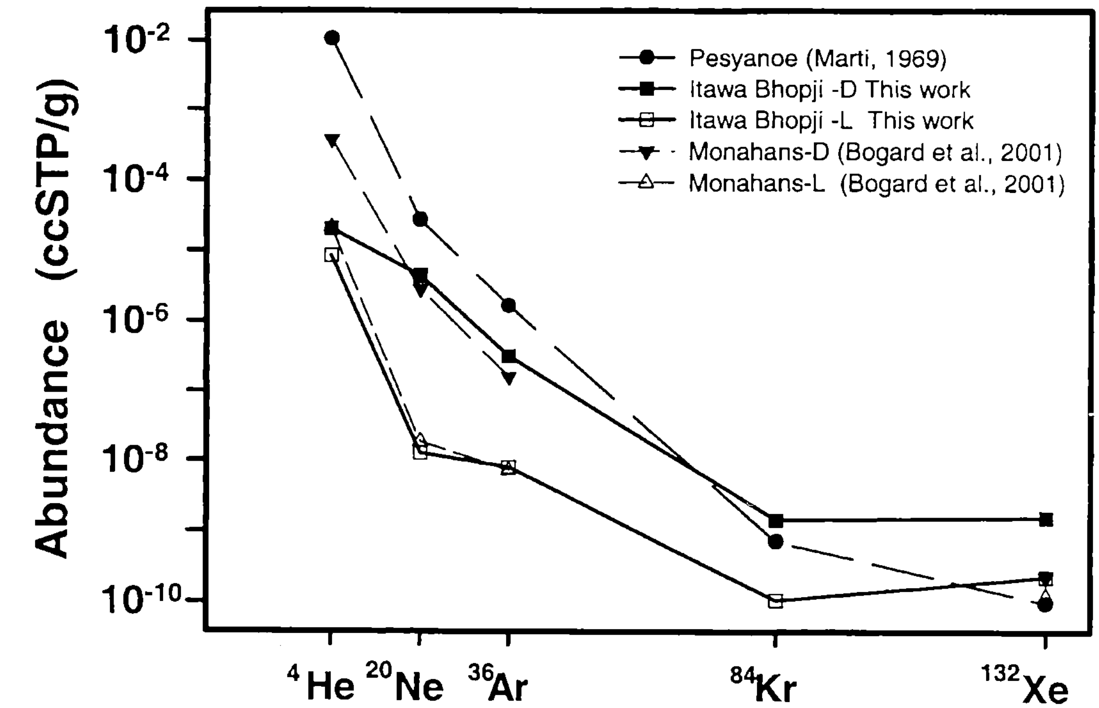

FIG. 7. Comparison of abundances of rare gases in light (L) and dark (D) phases of Itawa Bhopji meteorite with those of Pesyanoe and Monahans. The abundance patterns of the Itawa Bhopji-D and L are similar to those of Monahans-D and L, respectively. While in both cases only dark samples show similar pattern to Pesyanoe for ^{20}Ne and ^{36}Ar, the relative abundances of ^{84}Kr and ^{132}Xe are clearly different indicating less solar contribution for Kr and Xe.

Attributing all the excess ^{4}He (over cosmogenic) to the radiogenic component and using average U, Th contents of L chondrites (Wasson and Kallemeyn, 1988), we derive a U, Th-^{4}He age of 3.9 Ga. Adopting K content of 824 ppm (Table 2), we obtain K-Ar age of 2.37 Ga, much lower than the U,Th-^{4}He age. The difference may arise if a part of ^{4}He is trapped. To match the U,Th-^{4}He with K-Ar ages, ~840 × 10^{-8} ccSTP/g of ^{4}He has to be of trapped origin. About 0.9 × 10^{-8} ccSTP/g of ^{20}Ne and 0.8 × 10^{-12} ccSTP/g of ^{36}Ar of trapped origin are also seen in the light lithology sample.

Dark Lithology

Isotopic ratios of ^{20}Ne/^{22}Ne and ^{38}Ar/^{36}Ar as well as large amounts of ^{22}Ne and ^{36}Ar in the dark lithology indicate the presence of a significant trapped component. Surprisingly, however, ^{4}He is only ~70% more abundant in dark as compared to the light lithology. The peak Ne release at 1000 °C also shows the highest ^{20}Ne/^{22}Ne ratio of 11.95. Even the total Ne has ^{20}Ne/^{22}Ne = 10.97, characteristic of the solar component. In Fig. 7, we compare the trapped noble gas amounts for the light and dark lithologies of Itawa Bhopji with the trend shown by the gas-rich meteorite Pesyanoe (Marti, 1969). The data for Monahans, having solar gases and also bearing halites (Bogard *et al.*, 2001), is also shown for comparison. Though the presence of solar gases is clear from the trends in the dark lithologies, the absolute amounts (of ^{20}Ne and ^{36}Ar, for example) in both these meteorites are about an order of magnitude lower than in Pesyanoe. The trends for Itawa Bhopji and Monahans are parallel, except for He, indicating a severe He loss in Itawa Bhopji. Also, the ratio ^{84}Kr/^{132}Xe for both Itawa Bhopji and Monahans are much lower compared to

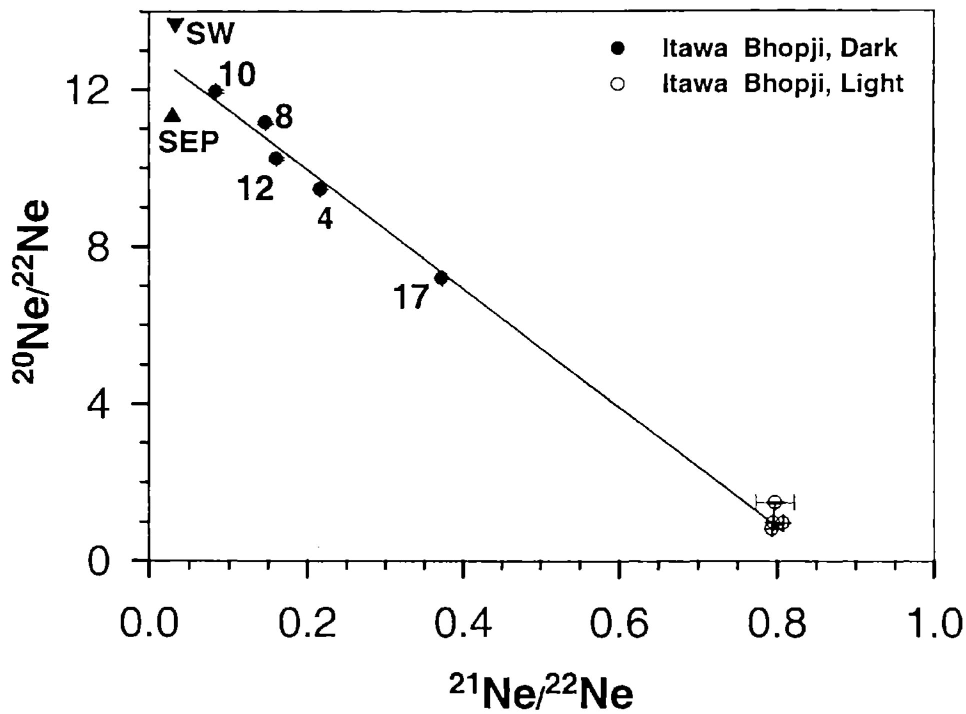

FIG. 8. Three-isotope plot ($^{20}Ne/^{22}Ne$ *vs.* $^{21}Ne/^{22}Ne$) showing the presence of solar component in the Itawa Bhopji meteorite. Numbers adjacent to the dark lithology data indicate temperature in hundreds of degrees Celsius. While all the light lithology data cluster around the cosmogenic end member with $(^{22}Ne/^{21}Ne)_c = 1.24$, the dark lithology data fall on the line joining the cosmogenic component and a trapped component. The linear regression line that includes data points for both lithologies intersects the line joining the solar wind (SW) and solar energetic particles (SEP) points at 12.50 ± 0.17.

Pesyanoe indicating that the solar component of Kr and Xe is minor in these two chondrites. Kr and Xe in both of them are largely dominated by normal "ordinary chondrite" (OC) component.

The Ne isotopic data are displayed in Fig. 8. The light lithology points form a cluster, defining the cosmogenic end member giving $(^{22}Ne/^{21}Ne)_c = 1.24$. The dark lithology points fall along a line joining the cosmogenic end member defined by the light lithology and a trapped component. The intersection of the line joining the solar wind and solar energetic particles points and the regression line through the dark lithology data gives the value of $(^{20}Ne/^{22}Ne)_T = 12.50 \pm 0.17$, a solar component (mixture of solar wind and solar energenic particles).

Assuming ^4He to be entirely due to trapped component, we calculate $(^4He/^{20}Ne)_T = 6.5$ which is very low compared to the solar ratio of ~400. The ^4He consists of cosmogenic, radiogenic, and trapped components, each of which can be estimated if we assume that the radiogenic component in both the lithologies (L and D) is comparable, both in concentration as well as in retentivity. Following this approach, we derive $^4He_T = 2010 \times 10^{-8}$ ccSTP/g and $(^4He/^{20}Ne)_T = 4.6$, much smaller than the value of ~400 expected for solar gases. This also implies a severe ^4He loss. The low K-Ar age of 2.37 Ga is also suggestive of gas loss. The $(^{20}Ne/^{36}Ar)_T = 13.9$ for the dark sample, though having a definite signature of the solar component, is less than the value of 40 expected for pure solar end member (Wieler, 1998). This observation again points to a loss of Ne in preference to Ar in a thermal or shock event subsequent to solar wind loading.

Exposure on Parent Body

Neutron-produced excesses of ^{36}Ar, ^{82}Kr and ^{128}Xe has been observed in both L and D lithologies which have been produced at a different stage of irradiation under heavy shielding so that significant ^{21}Ne is not produced (Murty and Mahajan, 2001).

The low ^{60}Co activity (~0.48 dpm/kg; Table 4), implies low neutron fluxes during the terminal part of the meteorite exposure in interplanetary space, which are inadequate to explain the observed neutron excess of ^{82}Kr and ^{128}Xe. Similar records of regolith irradiation have been identified in Monahans and Fermo H5 chondrite (Bogard *et al.*, 2001; Bonino *et al.*, 2001b). Hence, in addition to the brief irradiation of the dark lithology on the surface of the parent body wherein the solar gases are acquired, the Itawa Bhopji meteoroid had received an additional irradiation under heavy shielding on the parent body, wherein the neutron-capture-produced stable isotopes of ^{36}Ar, ^{82}Kr, ^{128}Xe from halogens were produced.

CONCLUSIONS

There have been unusual number of meteorite falls in Rajasthan, around the town of Jodhpur over the past decade.

Itawa Bhopji is the fifth recorded fall during the past decade (1991–2000). Based on the statistics of fall in India (117 known falls in 200 years; Ghosh and Dube, 1999), only one fall per decade is expected in Rajasthan. The five falls: Didwana (H5, 1991 August 12), Lohawat (howardite, 1994 October 30), Devri Khera (L5/6, 1994 October 30), Piplia Kalan (eucrite, 1996 June 20) and Itawa Bhopji (L3/5, 2000 May 30) belong to different classes, have different exposure ages (ranging between 8 and 110 Ma) (Bhandari *et al.*, 1998; Paliwal *et al*, 2001; Sisodia *et al.*, 2001) and are therefore not related to any specific asteroidal body or originated in any special collisional event in the asteroidal belt. Only two of them, Piplia Kalan and Lohawat, belonging to the howardite–eucrite–diogenite (HED) group could have possibly originated from a single body. Furthermore, Piplia Kalan (20.15 h), Didwana (22.00 h) and Lohawat (23.45 h) are late evening falls, whereas Itawa Bhopji is an early afternoon fall. The increased number of recoveries may be due to better awareness, but this is not a country-wide or global phenomenon. In the rest of India only three other falls have been recorded during this period (Vissannapeta, eucrite, 1997 December 13; Ghosh *et al.*, 2000 and Sabrum, 1999 April 30; Ghosh *et al.*, 2002). We therefore believe that increased number of falls in Rajasthan during the past decade is a statistical fluctuation, which needs to be investigated further.

Petrographic and chemical studies have shown that Itawa Bhopji is a L3-5 chondrite breccia. L type regolith breccias are relatively rare, forming only <1% of the known L chondrites in comparison to H chondrites where ~20% are brecciated. This meteorite therefore may be useful for studying regolith processes on the L-chondrite parent bodies such as deep burial, surface exposure, *etc.* The rare gas data reported here show a multi-stage exposure of the meteorite with deep burial on the parent body, where the neutron effects in rare gases were generated and a surface exposure, where solar gases were implanted, followed by a 19.6 Ma exposure in interplanetary space. During these exposures, significant amounts of He and some Ne were lost. The high track densities, low activity of radioisotopes produced due to spallation and extremely low neutron-capture radioisotope ^{60}Co (~0.48 dpm/kg) indicate a small meteoroid mass (~11 kg).

Acknowledgements–We thank Rajneesh Bhutani for his help in procuring the meteorite sample and Dr B. B. Arora for allowing us measurements on the main fragment. Our appreciation is due to Beth Ellen Clark and G. Bonino for useful comments which helped in improving the manuscript. We thank Clifford Lopate for providing the neutron monitor data collected under NSF grant ATM 99-12341. Part of this work was carried out under the National Planetary Science and Exploration Programme supported by Indian Space Research Organization. The efforts of K. R. Nambiar in preparation of the manuscript are appreciated.

Editorial handling: B. E. Clark

REFERENCES

BHANDARI N., GOSWAMI J. N., LAL D., MACDOUGALL D. AND TAMHANE A. S. (1972) A study of the vestigial records of cosmic rays in lunar rocks using a thick section technique. *Proc. Ind. Acad. Sci.* **534**, 27–50.

BHANDARI N., BHATTACHARYA S. K. AND SOMAYAJULU B. L. K. (1978) Cosmogenic radioisotopes in Dhajala chondrite: Implications to variations of cosmic ray fluxes in the interplanetary space. *Earth Planet. Sci. Lett.* **40**, 194–202.

BHANDARI N., LAL D., RAJAN R. S., ARNOLD J. R., MARTI K. AND MOORE C. B. (1980) Atmospheric ablation of meteorites: A study based on cosmic ray tracks and neon isotopes. *Nuclear Tracks* **4**, 213–262.

BHANDARI N., BONINO G., CALLEGARI E., CINI CASTAGNOLI G. C., MATHEW K. J., PADIA J. T. AND QUEIRAZZA G. (1989) The Torino, H6 meteorite shower. *Meteoritics* **24**, 29–34.

BHANDARI N. *ET AL.* (1993) Depth and size dependence of cosmogenic radionuclide production rates in stony meteoroids. *Geochim. Comochim. Acta* **57**, 2361–2375.

BHANDARI N., BONINO G., CINI CASTAGNOLI G. AND TARICCO C. (1994) The 11 year solar cycle variation of cosmogenic isotope production rates in chondrites (abstract). *Meteoritics* **29**, 443–444.

BHANDARI N., MURTY S. V. S., SUTHAR K. M., SHUKLA A. D., BALLABH G. M., SISODIA M. S. AND VAYA V. K. (1998) The orbit and exposure history of the Piplia Kalan eucrite. *Meteorit. Planet. Sci.* **33**, 455–461.

BHATTACHARYA S. K., GOSWAMI J. N. AND LAL D. (1973) Semiempirical rates of formation of cosmic ray tracks in spherical objects exposed in space: Preatmospheric and post atmospheric depth profiles. *J. Geophys. Res.* **78**, 8356-8363.

BOGARD D. D., NYQUIST L. E., BANSAL B. M., GARRISON D. H., WIESMAN H., HERZOG G. F., ALBRECHT A. A., VOGT S. AND KLEIN J. (1995) Neutron-capture ^{36}Cl, ^{41}Ca, ^{36}Ar and ^{150}Sm in large chondrites: Evidence for high fluences of thermalized neutrons. *J. Geophys. Res. (Planets)* **E5**, 9401–9416.

BOGARD D. D., GARRISON D. H. AND MASARIK J. (2001) The Monahans chondrite and halite: Argon-39/argon-40 age, solar gases, cosmic-ray exposure ages and parent body regolith neutron flux and thickness. *Meteorit. Planet. Sci.* **36**, 107–122.

BONINO G. AND CINI CASTAGNOLI G. (1997) Solar cycles recorded in meteorites. In *Past and Present Variability of the Solar-Terrestrial System: Measurements, Data Analysis and Theoretical Models* (eds. G. Cini Castagnoli and A. Provenzale), pp. 71–82. IOS Press, Amsterdam, The Netherlands.

BONINO G., CINI CASTAGNOLI G., CANE D., TARICCO C. AND BHANDARI N. (2001a) Solar modulation of the galactic cosmic ray spectra since the Maunder minimum. *Proc. Intern. Cosmic Ray Conf.* **27th**, 3769–3772.

BONINO G., BHANDARI N., MURTY S. V. S., MAHAJAN R. R., SUTHAR K. M., SHUKLA A. D., SHUKLA P. N., CINI CASTAGNOLI G. AND TARICCO C. (2001b) Solar and galactic cosmic ray records of the Fermo (H) chondrite regolith breccia. *Meteorit. Planet. Sci.* **36**, 831–839.

EUGSTER O. (1988) Cosmic ray production rates for ^{3}He, ^{21}Ne, ^{38}Ar, ^{82}Kr and ^{126}Xe in chondrites based on ^{81}Kr-Kr exposure ages. *Geochim. Cosmochim. Acta* **52**, 1649–1662.

EVANS J. C., REEVES, J. H., RANCITELLI L. A. AND BOGARD D. D. (1982) Cosmogenic nuclides in recently fallen meteorites: Evidence for galactic cosmic ray variations during the period 1967–1978. *J. Geophy. Res.* **87**, 5577–5591.

GHOSH S. AND DUBE A. (1999) *Pictorial Catalogue on One Hundred Indian Meteorites.* Geological Survey of India Catalogue Series No. 3, Geological Survey of India, Calcutta, India. 308 pp.

GHOSH S., PANT N. C., RAO T. K., RAMA MOHANA C., GHOSH J. B., SHOME S., BHANDARI N., SHUKLA A. D. AND SUTHAR K. M. (2000) The Vissannapeta eucrite. *Meteorit. Planet. Sci.* **35**, 913–917.

GHOSH S., MURTY S. V. S., PANT N. C., GHOSH J. B., SHOME S., SHUKLA A. D., MAHAJAN R. R., SHUKLA P. N. AND BHANDARI N.

(2002) Fall, classification and cosmogenic records of the Sabrum (LL6) chondrite. *Meteorit. Planet. Sci.* **37**, 439–448.

HEUSSER G., OUYANG Z., KIRSTEN T., HERPERS U. AND ENGLERT P. (1985) Conditions of the cosmic ray exposure of the Jilin chondrite. *Earth Planet. Sci. Lett.* **72**, 263–272.

KALLEMEYN G. W., RUBIN A. E., WANG D. AND WASSON J. T. (1989) Ordinary chondrites: Bulk composition, classification, lithophile element fractionations, and composition-petrographic type relationships. *Geochim. Cosmochim. Acta* **53**, 2747–2767.

KONG P. AND EBIHARA M. (1997) The origin and nebular history of the metal phase of ordinary chondrites. *Geochim. Cosmochim. Acta* **61**, 2317–2329.

KRISHNASWAMI S., LAL D., PRABHU N. AND TAMHANE A. S. (1971) Olivines: Revelation of tracks of charged particles. *Science* **174**, 287–292.

LAUL J. C. (1979) Neutron activation analysis of geological materials. *Atomic Energy Rev.* **17**, 603–695.

LEYA I., LANGE H-J., NEUMANN S., WIELER R. AND MICHEL R. (2000) The production of cosmogenic nuclides in stony meteoroids by galactic cosmic ray particles. *Meteorit. Planet. Sci.* **35**, 259–286.

LOCKWOOD M., STAMPER R. AND WILD M. N. (1999) A doubling of the Sun's coronal magnetic field during the past 100 years. *Nature* **399**, 437–439.

MARTI K. (1969) Solar-type xenon: A new isotopic composition of xenon in Pesyanoe meteorite. *Science* **166**, 1263–1265.

MARTI K. AND GRAF T. (1992) Cosmic ray exposure history of ordinary chondrites. *Ann. Rev. Earth Planet. Sci.* **20**, 211–243.

MURTY S. V. S. AND MAHAJAN R. R. (2001) Heavy nitrogen and nucleogenic Kr and Xe in Itawa Bhopji chondrite (abstract). *Meteorit. Plant. Sci.* **36 (Suppl.)**, A143–A144.

MURTY S. V. S., BHANDARI N., SUTHAR K. M., CLEMENT C. J., BONINO G. AND CASTAGNOLI C. (1998) Cosmogenic effects in Mbale L5/6 chondrite. *Meteorit. Planet. Sci.* **33**, 455–461.

PALIWAL B. S, MAHAJAN R. R, MURTY S. V. S., SHUKLA A. D., SHUKLA P. N., BHANDARI N., NATARAJAN R., HUTCHISON R., RUSSELL S. AND FRANCHI I. A. (2001) Chemical and isotopic characteristics of the Didwana-Rajod (H5) chondrite. *Meteorit. Planet. Sci.* **36**, 1249–1256.

POTDAR M. B. (1981) Nuclear interactions of the solar and galactic cosmic rays with interplanetary materials. Ph.D. thesis, Gujarat University, Ahmedabad, India. 214 pp.

RAMBALDI E. (1976) Trace element content of metals from L-group chondrites. *Earth Planet. Sci. Lett.* **31**, 224–238.

RAMBALDI E. R. (1977) The content of Sb, Ge and refractory siderophile elements in metals of L-group chondrites. *Earth Planet. Sci. Lett.* **33**, 407–419.

SHUKLA A. D., SHUKLA P. N., SUTHAR K. M., BHANDARI N., VAYA V. K., SISODIA M. S., SINHA ROY S., RAO K. N. AND RAJAWAT R. S. (1997) Piplia Kalan Eucrite: Fall, petrography and chemical characteristics. *Meteorit. Planet. Sci.* **32**, 611–615.

SHUKLA A. D., ADHYARU P. AND BHANDARI N. (2001) Highly sensitive γ-γ coincidence/anticoincidence spectrometer for measurement of low radioactivity in meteorites. In *Proceedings of Symposium on Nuclear Analytical and Radiochemistry* (NUCAR 2001), pp. 554–555. Bhabha Atomic Research Center, Mumbai, India.

SISODIA M. S., SHUKLA A. D., SUTHAR K. M., MAHAJAN R. R., MURTY S. V. S., SHUKLA P. N., BHANDARI N. AND NATARAJAN R. (2001) Lohawat howardite: Mineralogy, chemistry and cosmogenic effects. *Meteorit. Planet. Sci.* **36**, 1457–1466.

SOLANKI S. K., SCHÜSSLER M. AND FIGGE M. (2000) Evolution of the Sun's large-scale magnetic field since the Maunder minimum. *Nature* **408**, 445–447.

SOLAR GEOPHYSICAL DATA (2000) National Oceanic and Atmospheric Administration, **674**, Washington D.C., USA.

SPERGEL M. S., REEDY R. C., LAZARETH O. W., LEVY P. W. AND SLATEST L. A. (1986) Cosmogenic neutron-capture-produced nuclides in stony meteorites. *J. Geophys. Res.* **91**, D483–D494.

STÖFFLER D., KEIL K. AND SCOTT E. R. D. (1991) Shock metamorphism of ordinary chondrites. *Geochim. Cosmochim. Acta* **55**, 3845–3867.

VAN SCHMUS W. R. AND WOOD J. A. (1967) A chemical–petrologic classification for the chondritic meteorites. *Geochim. Cosmochim. Acta* **31**, 747–765.

WASSON J. T. AND KALLEMEYN G. W. (1988) Composition of chondrites. *Phil. Trans. Royal Soc. London* **A325**, 535–544.

WIELER R. (1998) The solar noble gas record in lunar samples and meteorites. *Space Sci. Rev.* **85**, 303–314.

WIELER R., BAUR H., PEDRONI A., SIGNER P. AND PELLAS P. (1989) Exposure history of the regolith chondrite Fayetteville: I. Solar-gas-rich matrix. *Geochim. Cosmochim. Acta* **53**, 1441–1448.

WIELER R. *ET AL.* (1996) Exposure history of the Torino meteorite. *Meteorit. Planet. Sci.* **31**, 265–272.